Optically Transparent Cathode for Dye-Sensitized Solar Cells Based on Graphene Nanoplatelets

Ladislav Kavan,[†,‡,*] Jun Ho Yum,[‡] and Michael Grätzel[‡]

[†]J. Heyrovský Institute of Physical Chemistry, v.v.i., Academy of Sciences of the Czech Republic, Dolejškova 3, CZ-18223 Prague 8, Czech Republic, and [‡]Laboratory of Photonics and Interfaces, Institute of Chemical Sciences and Engineering, Swiss Federal Institute of Technology, CH-1015 Lausanne, Switzerland

ABSTRACT Commercial graphene nanoplatelets in the form of optically transparent thin films on F-doped SnO_2 (FTO) exhibited high electrocatalytic activity toward I_3^-/I^- redox couple, particularly in electrolyte based on ionic liquid (Z952). The charge-transfer resistance, R_{CT}, was smaller by a factor of 5—6 in ionic liquid, compared to values in traditional electrolyte based on methoxypropionitrile solution (Z946). Optical spectra and electrochemical impedance confirm that the film's absorbance scales linearly with R_{CT}^{-1}. Electrocatalytic properties of graphene nanoplatelets for the I_3^-/I^- redox reaction are proportional to the concentration of active sites (edge defects and oxidic groups), independent of the electrolyte medium. Dye-sensitized solar cell (DSC) was assembled with this material as a cathode. Semitransparent (>85%) film of graphene nanoplatelets presented no barrier to drain photocurrents at 1 Sun illumination and potentials between 0 and *ca.* 0.3 V, but an order of magnitude decrease of R_{CT} is still needed to improve the behavior of DSC near the open circuit potential and, consequently, the fill factor. We predict that the graphene composite is a strong candidate for replacing both Pt and FTO in cathodes for DSC.

KEYWORDS: graphene · dye-sensitized solar cell · electrochemical impedance · ionic liquid · electrocatalysis

Dye-sensitized solar cells (DSCs), also called Grätzel cells, represent an attractive alternative of solid-state photovoltaics due to their high efficiency, low cost, and easy fabrication.[1,2] During the last two decades, considerable effort was focused on the optimization of photoanode material, dyes, and electrolytes, but less attention was paid to the counter electrode.[3,4] The latter is usually made from platinized F-doped SnO_2 (FTO). The reason is that Pt exhibits high electrocatalytic activity toward the iodide/triiodide redox couple, which is the common redox relay for most DSCs. Although the necessary amount of Pt on the cathode is very low, *ca.* 10—100 μg/cm^2,[3,5,6] there is a challenge for substituting platinum with a cheaper material. The request for Pt-free counter electrode is particularly important in solar cells which use other redox relays than I_3^-/I^-, such as quantum-dot-sensitized solar cell with a S^{2-}/S_x^{2-} couple in the electrolyte solution.[7] The palette of alternative materials comprises carbon, conducting polymers, polymer/Pt, or polymer/carbon composites (for review, see ref 4). Materials like Au, Cu_2S, and RuO_2 were also occasionally mentioned.[3,7,8] Recently, the high activities of surface-nitrided nickel[9] and CoS[10] were reported; the latter material is particularly attractive for fabricating optically transparent counter electrode on plastic substrates.

Carbon is the second most widely studied material for the DSC cathode after platinum. This research was triggered in 1996 by Kay and Grätzel,[11] who found good electrocatalytic activity of graphite/carbon black mixture. In subsequent years, various kinds of carbon were studied, such as hard carbon spherules,[12] activated carbon,[13] mesoporous carbon,[14] nanocarbon,[15] single-walled carbon nanotubes,[16] multi-walled carbon nanotubes (MWNTs),[17−20] and carbon black/TiO_2 composite.[21] The MWNTs were also assembled in composites with conducting polymer[17] and TiN.[22] (In the latter case, however, the presence of TiN requires further proof, due to possible mismatch of TiN with titanium oxynitrides at the used synthetic conditions.[23])

To achieve a comparable activity to platinum, carbon-based counter electrodes must have sufficiently high surface area. This requirement concurs the fact that the active sites for I_3^-/I^- redox reaction are defects and oxidic surface groups which are located at crystal edges of graphite.[4,21,24,25] Even so, carbonaceous electrodes which would be superior to Pt were reported only rarely for certain kinds of activated carbon.[13] Promising activity similar to that of Pt was also found for MWNT cathodes.[19,20,25] However, there is a debate in the literature

*Address correspondence to kavan@jh-inst.cas.cz.

Received for review September 2, 2010 and accepted November 23, 2010.

Published online December 3, 2010. 10.1021/nn102353h

whether or not the high activity of MWNTs comes, actually, from the residual metal or metal oxide catalyst particles which are present in the samples.[19,25,26]

In most cases, the carbon layers on the electrode were *ca.* 1−150 μm thick,[12−15,21,22] and they are, obviously, nontransparent to visible light. Optical transparency is, nevertheless, an important benefit of DSCs for certain practical applications, like windows, roof panels, or various decorative installations.[2] The transparent counter electrode is essential for the operation of plastic DSCs and for tandem solar cells.[2] In the case of solar cells which use conductive glass as the photocathode substrate, the optical transparency of counter electrode is not critical for the function of DSC, but it provides added value for practical applications as mentioned above. To the best of our knowledge, there is only one report on semitransparent DSCs with carbonaceous cathode, which was fabricated from MWNTs.[18] It exhibited good conversion efficiency of 7.59%, but direct comparison with Pt cathode was not made in this paper.

Hence, there is a challenge for further search and optimization of transparent Pt-free cathodes. Graphene seems to be an attractive material for this purpose because it forms transparent, conductive, and stretchable thin-film electrodes.[27−29] Müllen *et al.*[30] have used graphene as a collector layer of TiO_2 photoanode in dye-sensitized solar cell based on spiro-OMeTAD hole conductor. The layer had a conductivity of 550 S/cm and transparency of more than 70% within the 1000−3000 nm wavelengths region, but it dropped down to *ca.* 50% at 400 nm. Recently, Zhang *et al.*[31] reported on graphene nanosheet cathode for DSC, but the solar conversion efficiencies were only between 0.71 and 2.94%, depending on the calcination temperature (from 350 to 450 °C). Analogously, Choi *et al.*[32] reported on a rather poor performance of graphene cathode, but a composite of graphene with MWNTs exhibited enhanced activity, giving 3% solar conversion efficiency in DSCs. Recently, Roy-Mayhew *et al.*[33] reported on functionalized graphene sheets for the DSC cathode either on FTO or on mylar supports and found efficiencies of 5 or 3.8%, respectively, but their cathodes were, presumably, not transparent optically. In all cases,[30−33] graphene was prepared from chemically exfoliated graphene oxide *via* subsequent thermal treatment.

Perfect graphene does not seem to be the right candidate for a DSC cathode, in view of the limited number of active sites for I_3^-/I^- electrocatalysis.[4,21,25] This expectation comes from the fact that also the activity of basal-plane graphite is known to be low.[24] Nevertheless, small graphene nanoplatelets might behave differently if they have large number of active edge sites.[31−33] Such a defect-rich graphene seems to be favored over MWNTs for a transparent DSC cathode because the amount of active sites per one π-electron in carbonaceous skeleton is larger. (MWNTs are handicapped by the fact that the inner tubes hardly contribute to electrochemical activity, but absorb light.) Here we report one promising electrode material, which is both optically transparent and reasonably active for the I_3^-/I^- redox reaction. In contrast to earlier reports,[31−33] we obtained good solar conversion efficiency (≈5%) in DSCs with an optically transparent graphene cathode. The cathode was fabricated by drop-casting on FTO from non-optimized graphene nanoplatelets as-received from the producer.

RESULTS AND DISCUSSION

The basic requirements for electrocatalytic activity of the DSC cathode are outlined by the typical current densities on TiO_2 photoanode, which are *ca.* 20 mA/cm^2 under full Sun illumination.[2] Ideally, the exchange current density on the cathode, j_0, should be comparable, which provides an estimate of the required charge-transfer resistance, R_{CT}, of the cathode. From the equation

$$j_0 = \frac{RT}{nFR_{CT}} \quad (1)$$

this translates into R_{CT} of *ca.* 1.3 Ωcm^2. Such values are accessible for platinized FTO[6,21,34] (although they strongly depend on the Pt deposition method and electrolyte type[34]) as well as for massive carbon layers (≈20 μm thickness[15,21] or *ca.* 0.3 mg/cm^2).[14] We should note, however, that the reported R_{CT} values for carbon are usually normalized to the projected geometric area of the electrode. If we recalculate the charge-transfer resistances to the total surface area of carbon, we get R_{CT} values of *ca.* 5−25 kΩcm^2 for the same electrodes.[21] Trancik *et al.*[25] have suggested that the target carbonaceous film, which would, eventually, replace Pt@FTO, should have the following parameters: 80% optical transparency at a wavelength of 550 nm, R_{CT} of 2−3 Ωcm^2, and sheet resistance of 20 Ω/sq. Such a film has not yet been demonstrated experimentally.

The behavior of our reference system, that is, Pt@FTO, is demonstrated in Figure 1. The left panel of Figure 1 displays a cyclic voltammogram of a symmetrical sandwich cell with Z946 electrolyte. The electrolyte solution (coded Z946) is 1 M 1,3-dimethylimidazolium iodide + 0.15 M iodine + 0.5 M *N*-butylbenzoimidazole + 0.1 M guanidine thiocyanate in 3-methoxypropionitrile.[35] (For molecular formulas of the electrolyte components, see Supporting Information.) We observe an almost perfect ohmic response between −1 and 1 V bias. However, closer inspection reveals that the freshly assembled cell has higher currents than the cell after several days of aging. The changes were pronounced during the first 11 days; after this period, the cell was in a steady state with no marked aging changes within the next 10 days. Hauch and Georg[34] mentioned a poisoning of Pt, which might be respon-

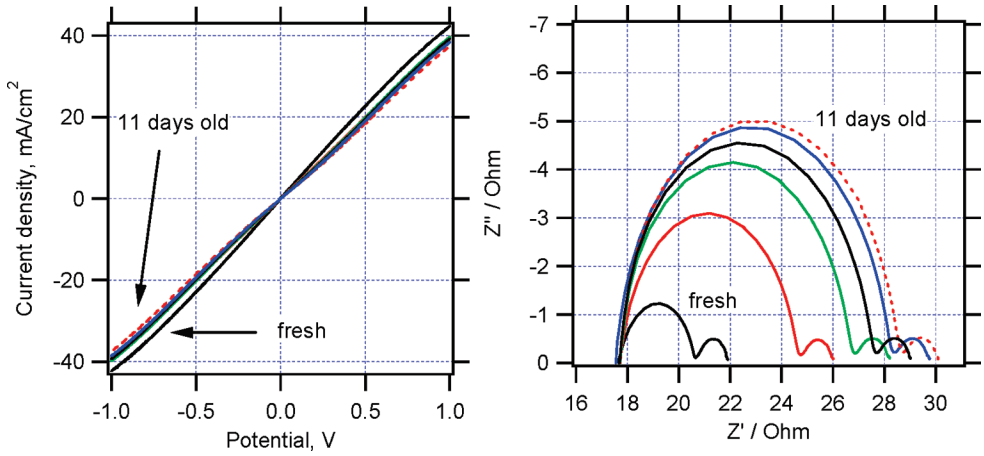

Figure 1. Left chart: cyclic voltammogram of a closed dummy cell with platinized FTO electrodes, scan rate 50 mV/s; electrolyte Z946. Right chart: Nyquist plot of electrochemical impedance spectra measured from 65 kHz to 0.1 Hz on a closed dummy cell with Pt@FTO electrodes; electrolyte Z946.

sible for this initial deactivation. Clearer manifestation of the poisoning effect is provided by the impedance spectra shown on Figure 1, right panel.

Electrochemical impedance of the symmetrical dummy cell can be fitted to a Randles-type circuit (R_{CT} with a parallel double-layer capacitance, C_{dl}) plus a series resistance, R_s, and the Nernst diffusion impedance, Z_N, in the electrolyte. The latter is related to the diffusion coefficient of I_3^- in the electrolyte solution, D_I:

$$Z_N = \frac{kT}{An^2e_0^2c\sqrt{i\omega}}\tanh\left(\sqrt{\frac{0.25i\omega}{D_IL}}\right) \qquad (2)$$

where A is the electrode area, c is the concentration of I_3^-, and L is the distance between electrodes.[34]

If the reactions at both electrodes are identical, we can simplify, according to Kirhoff's laws, our system to the equivalent circuit shown in Figure 2 with R_{CT} doubled and C_{dl} halved.[34] However, more accurate analysis points to a small deviation from the ideal capacitance, caused by the roughness of the electrodes.[5,14,21,22,34] Hence, the capacitance ($1/2C_{dl}$) should be replaced by a constant phase element (CPE) with an impedance Z_{CPE}:

$$Z_{CPE} = B(i\omega)^{-\beta} \qquad (3)$$

where B and β are frequency-independent parameters of CPE ($0 \leq \beta \leq 1$; for $\beta = 1$, the Z_{CPE} transforms into C_{dl}). The experimental impedance spectra for platinized FTO (Figure 1, right panel) are dominated by the RC element of the Pt/electrolyte interface in the high-frequency domain. They can be fitted to an almost ideal capacitance, with the CPE exponent β being about

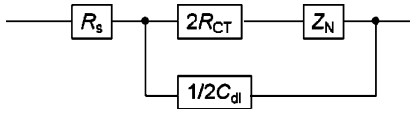

Figure 2. Equivalent circuit diagram for fitting the electrochemical impedance spectra of a dummy cell with two identical electrodes.

0.99 for all spectra. The found impedance parameters in Z946 electrolyte were as follows: $R_s = 18\ \Omega$, $R_{CT} = 0.4\ \Omega \cdot cm^2$, $C_{dl} = 18\ \mu F/cm^2$ (fresh electrode) and $R_s = 17\ \Omega$, $R_{CT} = 1.9\ \Omega \cdot cm^2$, $C_{dl} = 17\ \mu F/cm^2$ (electrode after 11 days of aging). The impedance of ionic diffusion is expressed by the second semicircle in the low-frequency domain (Figure 1, right chart). As expected, it does not depend on electrode aging because ionic diffusion in the electrolyte solution (eq 2) is invariant with the surface conditions at electrodes.

Figure 3 presents the electrochemical behavior of symmetrical dummy cells with graphene electrodes (G1 to G5) having different amounts of graphene nanoplatelets deposited on FTO. The G1−G5 electrodes were prepared by drop-casting from isopropyl alcohol suspension of graphene nanoplatelets (see Experimental Section for details). The left panel in Figure 3 shows the cyclic voltammograms in Z946 electrolyte, and for comparison also, the corresponding voltammogram of pure FTO electrode is plotted for reference. Obviously, there is a considerable overpotential for the I_3^-/I^- couple, but the currents increase with increased graphene loading, that is, from G1 to G5. Again, this is more clearly reflected by impedance analysis shown in Figure 3 (right panel) and by the fitted data summarized in Table 1. In this case, we cannot distinguish Z_N as in

TABLE 1. Electrochemical Impedance Parameters of the Studied Graphene-Based Cathodes

electrode	electrolyte	R_s (Ω)	R_{CT} ($\Omega \cdot cm^2$)	CPE:B ($S.s^\beta$)	CPE:β
G1	Z946	23	1183	8.6×10^{-5}	0.89
G2	Z946	26	590	9.1×10^{-5}	0.92
G3	Z946	29	308	1.1×10^{-4}	0.91
G4	Z946	28	134	3.4×10^{-4}	0.87
G5	Z946	31	94	5.0×10^{-4}	0.91
G1	Z952	28	205	1.0×10^{-4}	0.89
G2	Z952	27	118	1.5×10^{-4}	0.80
G3	Z952	30	50	2.1×10^{-4}	0.88
G4	Z952	29	22	4.0×10^{-4}	0.89
G5	Z952	29	15	9.4×10^{-4}	0.84

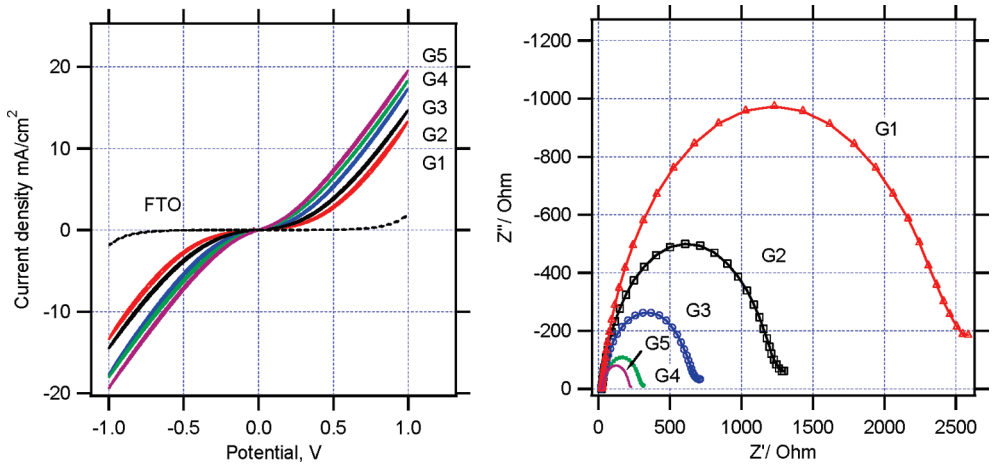

Figure 3. Left chart: cyclic voltammogram of a dummy cell with graphene on FTO electrodes (G1 to G5), scan rate 50 mV/s, electrolyte Z946. Right chart: Nyquist plot of electrochemical impedance spectra measured from 65 kHz to 0.1 Hz on dummy cell with graphene on FTO electrodes (G1 to G5); electrolyte Z946.

the case of platinized FTO (Figure 1). The series resistance, R_s, is larger for graphene electrodes and approaches the value of platinized FTO only for the smallest graphene loading (G1). The same effect was observed also for carbon black.[21] We may note that the CPE parameter B is proportional to R_{CT}, which shows that the improved electrocatalytic activity is simply related to the active surface area of our graphene nanoplatelets. Recently, Roy-Mahew *et al.*[33] upgraded the traditional equivalent circuit (Figure 2) by adding the Nernst diffusion impedance within electrode pores in functionalized graphene sheets. In our case, the diffusion in pores can obviously be neglected because the amount of graphene on FTO is small.

Interestingly, our graphene films exhibit significantly higher electrochemical activity in the electrolyte based on ionic liquid. This electrolyte (coded Z952) is a solvent-free mixture of 1,3-dimethylimidazolium iodide + 1-ethyl-3-methylimidazolium iodide + 1-ethyl-3-methylimidazolium tetracyanoborate + iodine + *N*-butylbenzoimidazole + guanidinium thiocyanate.[36] (For molecular formulas of the electrolyte components, see Supporting Information.) Figure 4 (left chart) shows cyclic voltammograms of three electrodes, G3, G4, and G5, in this electrolyte. (These electrodes are duplicates of the electrodes presented in Figure 3 above.) Also shown is the voltammogram of platinized FTO. The latter voltammogram confirms that there is a limiting current density of *ca.* 10 mA/cm^2, which is controlled by the mass transport in our ionic liquid electrolyte. We may note that there is almost no marked overpotential for the I_3^-/I^- couple on our film G5, which behaves almost like platinized FTO (Figure 4).

Right chart in Figure 4 shows the corresponding impedance spectra. To demonstrate the improvement in electrochemical parameters, the impedance spectra in Z946 and Z952 electrolytes are compared in Figure 4 (dashed *vs* full curves). We should note a similarity of the Z946 impedance spectra plotted in Figure 4 (dashed curves) and those in Figure 3 (electrodes G3−G5). As different films were tested in Figures 3 and 4, this comparison proves that our graphene deposition technique (see Experimental Section) is reasonably reproducible. More importantly, the charge-transfer resistance, R_{CT}, is smaller by a factor of about 5−6 in the ionic liquid medium (Z952) compared to usual electrolyte solution (Z946); the actual values are summarized in Table 1.

The reason for such a striking improvement of R_{CT} for graphene/ionic liquid interface is not clear at this stage of research. Hausch and Georg[34] found that R_{CT} grew with the viscosity of solvent and the size of solvent molecule for Pt@FTO in various electrolyte solutions. Obviously, the argument about viscosity control of R_{CT} is just opposite of what we have observed. In general, the I_3^-/I^- redox reaction in electrolyte solutions assumes two mechanistic models: (i) the electroactive ions (I_3^- or I^-) first discard the solvating molecules, migrate through the double layer, adsorb on the electrode, and transfer electron in "naked state"; or (ii) the electroactive ions (I_3^- or I^-) remain in solvated state during the charge-transfer process, and the redox reaction occurs *via* electron tunneling through the solvating sphere.[34] In the absence of any solvent, like in ionic liquids, both of these barriers for electron transfer are missing. Hence the solvation, rather than viscosity, seems to be the decisive parameter controlling our reaction.

Independent of the electrolyte medium used, the activity of our electrodes depends on the amount of graphene nanoplatelets deposited on FTO support. This conclusion is further corroborated by optical spectra of our G1−G5 films (Figure 5, left panel). Similarly to large-scale CVD-grown graphene films,[27] the featureless transmittance curve drops toward shorter wavelengths. The transmittance of our G1 film roughly corresponds to the transmittance of a perfect bilayer graphene.[28] Interestingly, there is a linear fit between

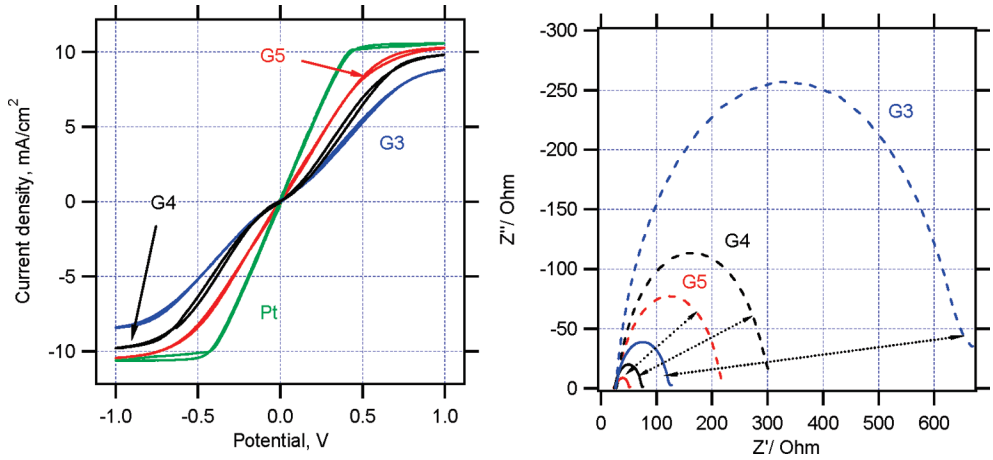

Figure 4. Electrochemical behavior of graphene electrodes in ionic liquid electrolyte (Z952) and in volatile electrolyte (Z946). The electrodes (G3, G4, G5) were duplicates of the corresponding electrodes shown in Figure 3. Left chart: cyclic voltammogram of a dummy cell with graphene on FTO electrodes, scan rate 5 mV/s, electrolyte Z952. The voltammogram of platinized FTO is also shown for comparison. Right chart: Nyquist plot of electrochemical impedance spectra measured from 65 kHz to 0.1 Hz on dummy cell with graphene on FTO electrodes. Dashed curves: electrolyte Z946, full curves: electrolyte Z952.

the absorbance of our electrodes ($-\log T_\lambda$, where T_λ is transmittance at the given wavelength, λ) and the inverse charge-transfer resistance, $1/R_{CT}$, both in volatile electrolyte solution (Z946) and in ionic liquid (Z952). This is demonstrated on Figure 5 (right panel) for absorbance at an arbitrarily chosen wavelength of $\lambda = 500$ nm. As the absorbance is, according to Lambert−Beer law, proportional to concentration, we may conclude that there is a simple proportionality between $1/R_{CT}$ and the concentration of active sites for the I_3^-/I^- electrocatalytic exchange, *viz.* defects and oxidic surface groups at crystal edges.[4,21,24,25] Obviously, for a semitransparent DSC cathode, a compromise has to be sought between the optical transparency and electrochemical activity. This task is reminiscent of similar problems with MWNTs.[18,25]

Finally, we tested the performance of our medium-loaded graphene cathode (G3) in a DSC. Figure 6 and Table 2 show the corresponding current−voltage characteristics for a reference DSC with platinized cathode and G3 cathode under various light intensities. The short circuit photocurrents densities (j_{SC}) are almost identical for both cathodes independent of the light intensity and electrolyte medium. Also we may note that the j_{SC} on G3 in ionic liquid at 1 Sun (*ca.* 11 mA/cm^2) is similar to the transport-limited current densities observed for Pt in a symmetrical dummy cell (Figure 4), despite the fact that the cell geometry and other experimental parameters are quite different in both cases. Hence, graphene cathode presents no barrier for the maximal current, which is achievable in the solar cell under 1 Sun illumination at potentials between 0 and *ca.* 0.3 V. The dark current in DSC with the graphene cathode is considerably smaller at potentials positive to *ca.* 0.6 V (Figure 6), but deeper discussion of this difference is beyond the scope of this paper. The larger

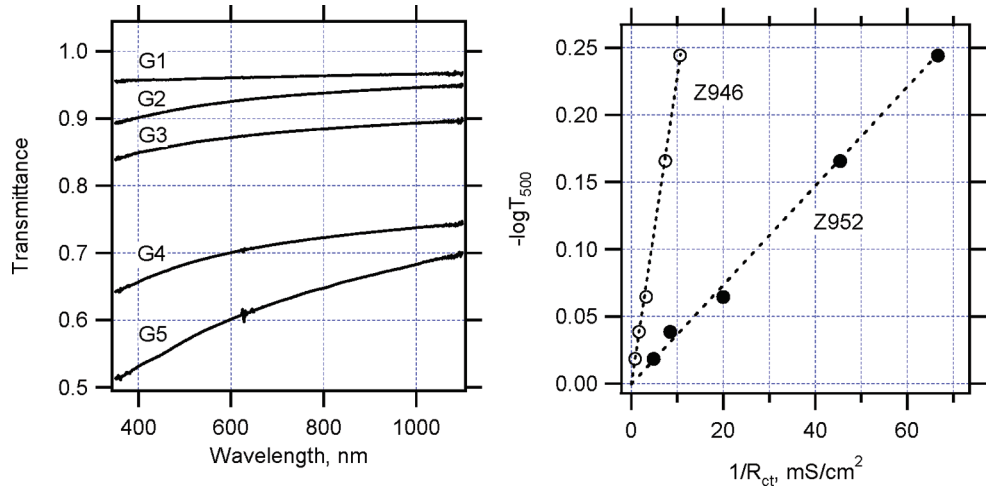

Figure 5. Left chart: Optical transmittance spectra of graphene films (G1 to G5) deposited on glass. Right chart: Optical absorbance at a wavelength of 500 nm plotted as a function of inverse charge-transfer resistance determined from electrochemical impedance spectra in volatile electrolyte, Z946 (open points), and in ionic liquid electrolyte, Z952 (solid points).

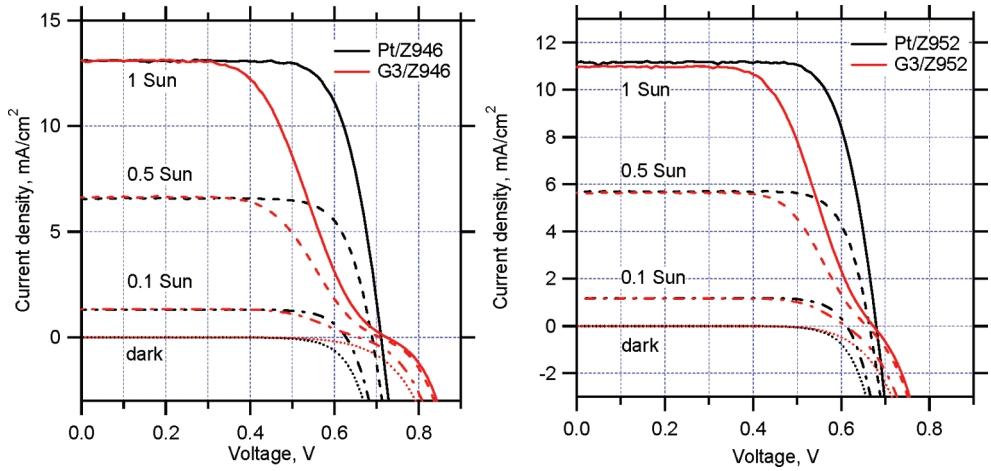

Figure 6. Current−voltage characteristics of a dye-sensitized solar cell with the platinized FTO (black lines) or G3 cathode (red lines) under various light intensities. Left chart: Z946 electrolyte. Right chart: Z952 electrolyte.

charge-transfer resistance of G3 influences particularly the *j*−*V* curves near the open circuit potential. This decreases the fill factor, predominantly at higher light intensities. The actual data are collected in Table 2.

In accord with the electrochemical data discussed above, the graphene cathode exhibits markedly better performance in DSC with ionic liquid (Z952) due to the lower R_{CT} in this medium (Figure 6, right chart). At 1 Sun illumination, the cell with the G3 electrode yielded the efficiency of 4.4% and fill factor of 0.60 when compared to platinized electrode, 5.7% and 0.75. The relatively higher fill factor, 0.65 and 0.73 (*vs* 0.57 and 0.65 with Z946), was also observed at lower light intensities, 0.5 and 0.1 Sun, respectively (Table 2). Our efficiencies compare favorably to those in earlier reports on DSCs with a graphene-based cathode.[31−33] Since our G3 was selected here as a non-optimized example of medium-loaded electrode, these results are encouraging in view of further engineering of graphene cathodes for DSC. Our G3 film had a transmittance better than 85% in the visible spectrum (Figure 5), but its R_{CT} still needs to be decreased by a factor of *ca.* 10 to make it competitive to platinized FTO. The final goal would be a FTO- *and* Pt-free cathode for DSC. For instance, a combination of defect-free graphene as a current collector (*cf.* Müllen *et al.*[30]) with highly active graphene nanoplatelets as a catalyst might, eventually, meet the criteria of carbonaceous DSC cathode, formulated by Trancik *et al.*[25]

TABLE 2. Characteristics of Solar Cells with N-719 Sensitized TiO_2 Photoanode and Pt or G3 Cathodes under Various Light Intensities (I_0): Short Circuit Photocurrent Density = j_{SC}, Open Circuit Voltage = V_{OC}, Fill Factor = FF, Solar Conversion Efficiency = η

electrolyte	cathode	I_0 (Sun)	j_{SC} (mA/cm^2)	V_{OC} (mV)	FF	η (%)
Z946	Pt	1	13.1	711	0.74	6.89
Z946	Pt	0.5	6.58	689	0.76	6.88
Z946	Pt	0.1	1.31	627	0.77	6.33
Z946	G3	1	13.1	724	0.52	5.00
Z946	G3	0.5	6.64	708	0.57	5.38
Z946	G3	0.1	1.34	657	0.65	5.73
Z952	Pt	1	11.2	679	0.75	5.70
Z952	Pt	0.5	5.71	663	0.77	5.84
Z952	Pt	0.1	1.18	612	0.78	5.70
Z952	G3	1	11.0	673	0.60	4.38
Z952	G3	0.5	5.64	658	0.65	4.81
Z952	G3	0.1	11.6	610	0.73	5.16

CONCLUSIONS

Graphene nanoplatelets exhibit promising electrocatalytic activity toward I_3^-/I^- redox couple in thin films which are optically semitransparent. The charge-transfer resistance, R_{CT}, is smaller by a factor of 5−6 in ionic liquid electrolyte (Z952) compared to that in traditional electrolyte in methoxypropionitrile solution (Z946). The difference was attributed to solvation-related events rather than viscosity control of the charge-transfer mechanism.

In both electrolytes tested (Z946, Z952), the R_{CT} scaled linearly with the graphene film's absorbance, confirming a simple proportionality between the concentration of active sites (edge defects and oxidic groups) and electrocatalytic properties of the electrode for I_3^-/I^- redox reaction.

Solar efficiency tests confirmed that semitransparent film of graphene nanoplatelets presented no barrier to drain photocurrents at 1 Sun illumination and potentials between 0 and *ca.* 0.3 V.

Consistent with the impedance data on symmetrical dummy cells, the graphene cathode exhibited better performance in DSC with ionic liquid electrolyte (Z952). Nevertheless, the R_{CT} of graphene nanoplatelets still needs to be decreased *ca.* 10 times to improve the behavior of DSC near the open circuit potential and, consequently, the fill factor.

Our study points at an optimistic prediction that all-carbon cathode (FTO- and Pt-free) is eventually accessible from graphene composites.

EXPERIMENTAL SECTION

Materials. Graphene nanoplatelets, grade 3, were purchased from Cheap Tubes, Inc. (USA). According to the manufacturer's specification, they consisted of several sheets of graphene with an overall thickness of approximately 5 nm (ranging from 1 to 15 nm) and particle diameters less than 2 μm, surface area of 600−750 m^2/g. The platelets were dispersed in 2-propanol by a short sonication (*ca.* 1 min), and the dispersions (0.1−2 mg/mL) were stable for several days without marked sedimentation. This solution was drop-casted (*ca.* 0.1 mL/cm^2) on FTO glass (TEC 15 from Libbey-Owens-Ford, 15 Ω/sq), and a uniform semitransparent film was obtained after drying at room temperature. Five different films (G1−G5) were prepared by varying amounts of graphene on FTO. The graphene loading was adjusted by varying the concentration of the used dispersion (0.1−2 mg/mL) and/or by repeating the drop-cast deposition. The supporting FTO sheet was 2.5 × 1 cm^2, but the active carbon-coated layer was 1 cm^2, leaving the edge for the electrical contact. The latter was fabricated by ultrasonic soldering (Cerasolzer alloy 246, MBR Electronics GmbH). For optical measurements, the same graphene films were also duplicated by deposition on microscope glass sheets to avoid interference fringes coming from the FTO layer. Platinized FTO was prepared by deposition of *ca.* 5 μL/cm^2 of 10 mM H_2PtCl_6 in 2-propanol and calcination at 400 °C for 15 min.[8,21]

To investigate the cathode's performance at conditions which are as close as possible to the actual situation in DSC, the symmetrical sandwich cell was used.[34] It was fabricated from two identical FTO sheets which were separated by 70 μm thick Surlyn (DuPont) tape serving as a spacer leaving 1 × 1 cm^2 active area with two edges of the cell open for electrolyte soaking. The aging of platinized FTO electrodes was studied in a geometry identical to that of ordinary DSC, that is, in a closed sandwich cell. In this case, the cell had circular active area of 0.38 cm^2 and was thermally sealed with 25 μm Surlyn foil. The cell was filled with an electrolyte through a hole in one FTO electrode and was finally closed by a Surlyn seal. The electrolyte solution was 1 M 1,3-dimethylimidazolium iodide + 0.15 M iodine + 0.5 M *N*-butylbenzoimidazole + 0.1 M guanidine thiocyanate in 3-methoxypropionitrile (coded Z946).[35] Alternatively, a solvent-free electrolyte based on ionic liquids was also used, Z952: 1,3-dimethylimidazolium iodide + 1-ethyl-3-methylimidazolium iodide + 1-ethyl-3-methylimidazolium tetracyanoborate + iodine + *N*-butylbenzoimidazole + guanidinium thiocyanate (molar ratio 12/12/16/1.67/3.33/0.67).[36] For photoelectrochemical tests, the mesoporous anatase TiO_2 film (20 nm particle size, 10 μm film thickness, 60% porosity) was sensitized with N-719 dye.[37] The DSC was assembled with a counter electrode using a Surlyn tape (25 μm in thickness) as a seal and spacer (see above). The cell active area for illumination was 0.2 cm^2, defined by a mask.

Methods. Electrochemical measurements were carried out using the PAR 273 potentiostat (EG&G) interfaced to a Solatron 1260A frequency response analyzer and controlled by CorrWare program. Electrochemical impedance data were processed using Zplot/Zview software. The impedance spectra were acquired in the frequency range from 65 kHz to 0.1 Hz, at 0 V bias voltage, and the modulation amplitude was 10 mV. The optical spectra were measured by Hewlett-Packard 8453 diode array spectrometer. For photoelectrochemical tests, the light source was a 450 W xenon light source (Osram XBO 450, Germany) with a filter (Schott 113). The light power was regulated to the AM 1.5G solar standard by using a reference Si photodiode equipped with a color-matched filter (KG-3, Schott) to reduce the mismatch in the region of 350−750 nm between the simulated light and AM 1.5G to less than 4%. The differing intensities were regulated with neutral wire mesh attenuator. The applied potential and cell current were measured using a Keithley model 2400 digital source meter.

Acknowledgment. This work was supported by the Czech Ministry of Education, Youth and Sports (Contract No. LC-510), by the Academy of Sciences of the Czech Republic (Contracts IAA 400400804 and KAN 200100801), by the EC 7th FP project Orion (Contract No. NMP-229036), and by the FP7-Energy-2010-FET project Molesol (Contract No. 256617). M.G. is very grateful to the European Research Council (ERC) for supporting of his research under the ERC-2009-AdG Grant No. 247404 MESOLIGHT. J.H.Y. acknowledges the support from the Korea Foundation for International Cooperation of Science & Technology through the Global Research Lab. We thank Dr. Shaik M. Zakeeruddin and Mr. Pascal Comte for their kind assistance.

Supporting Information Available: Molecular formulas of components in the Z946 and Z952 electrolytes. This material is available free of charge *via* the Internet at http://pubs.acs.org.

REFERENCES AND NOTES

1. Grätzel, M. Photoelectrochemical Cells. *Nature* **2001**, *414*, 338–344.
2. Kalyanasundaram, K. *Dye Sensitized Solar Cells*; EPFL Press & CRC Press: Lausanne, Switzerland, 2010.
3. Papageorgiou, N. Counter-Electrode Function in Nanocrystalline Photoelectrochemical Cell Configurations. *Coord. Chem. Rev.* **2004**, *248*, 1421–1446.
4. Murakami, T. N.; Grätzel, M. Counter Electrodes for DSC: Application of Functional Materials as Catalysts. *Inorg. Chim. Acta* **2008**, *361*, 572–580.
5. Liberatore, M.; Decker, F.; Burtone, L.; Zardetto, V.; Brown, T. M.; Reale, A.; Di Carlo, A. Using EIS for Diagnosis of Dye-Sensitized Solar Cells Performance. *J. Appl. Electrochem.* **2009**, *39*, 2291–2295.
6. Chen, C. M.; Chen, C. H.; Wei, T. C. Chemical Deposition of Platinum on Metallic Sheets as Counterelectrodes for Dye-Sensitized Solar Cells. *Electrochim. Acta* **2010**, *55*, 1687–1695.
7. Zhang, Q.; Zhang, Y.; Huang, S.; Huang, X.; Luo, Y.; Meng, Q.; Li, D. Application of Carbon Counterelectrode on CdS Quantum Dot-Sensitized Solar Cells. *Electrochem. Commun.* **2010**, *12*, 327–330.
8. Papageorgiou, N.; Maier, W. E.; Grätzel, M. An Iodine/Triiodide Reduction Electrocatalyst for Aqueous and Organic Media. *J. Electrochem. Soc.* **1997**, *144*, 876–884.
9. Jiang, Q. W.; Li, G. R.; Liu, S.; Gao, X. P. Surface-Nitrided Nickel with Bifunctional Structure as Low-Cost Counter-Electrode for Dye Sensitized Solar Cells. *J. Phys. Chem. C* **2010**, *114*, 13397–13401.
10. Wang, M.; Anghel, A. M.; Marsan, B.; Cevey Ha, N. L.; Pootrakulchote, N.; Zakeeruddin, S. M.; Grätzel, M. CoS Supersedes Pt as Efficient Electrocatalyst for Triiodide Reduction in Dye Sensitized Solar Cells. *J. Am. Chem. Soc.* **2009**, *131*, 15976–15977.
11. Kay, A.; Grätzel, M. Low Cost Photovoltaic Modules Based on Dye Sensitized Nanocrystalline Titanium Dioxide and Carbon Powder. *Sol. Energy Mater. Sol. Cells* **1996**, *44*, 99–117.
12. Huang, Z.; Liu, X.; Li, K.; Li, D.; Luo, Y.; Li, H.; Song, W.; Chen, L.; Meng, Q. Application of Carbon Materials as Counter Electrodes of Dye Sensitized Solar Cells. *Electrochem. Commun.* **2007**, *9*, 596–598.
13. Imoto, K.; Takahashi, K.; Yamaguchi, T.; Komura, T.; Nakamura, J.; Murata, K. High-Performance Carbon Counter Electrode for Dye Sensitized Solar Cells. *Sol. Energy Mater. Sol. Cells* **2003**, *79*, 459–469.
14. Wang, G.; Xing, W.; Zhou, S. Application of Mesoporous Carbon to Counter Electrode for Dye Sensitized Solar Cells. *J. Power Sources* **2009**, *194*, 568–573.
15. Ramasamy, E.; Lee, W. J.; Lee, D. Y.; Song, J. S. Nanocarbon Counterelectrode for Dye Sensitized Solar Cells. *Appl. Phys. Lett.* **2007**, *90*, 173103.
16. Suzuki, K.; Yamaguchi, M.; Kumagai, M.; Yanagida, S. Application of Carbon Nanotubes to Counter Electrodes of Dye Sensitized Solar Cells. *Chem. Lett.* **2003**, *32*, 28–29.
17. Fan, B.; Mei, X.; Sun, K.; Ouyang, J. Conducting Polymer/Carbon Nanotube Composite as Counter Electrode of Dye Sensitized Solar Cells. *Appl. Phys. Lett.* **2008**, *93*, 143103.
18. Ramasamy, E.; Lee, W. J.; Lee, D. Y.; Song, J. S. Spray Coated Multiwall Carbon Nanotube Counter Electrode for

Triiodide Reduction in Dye Sensitized Solar Cells. *Electrochem. Commun.* **2008**, *10*, 1087–1089.
19. Lee, W. J.; Ramasamy, E.; Lee, D. Y.; Song, J. S. Efficient Dye Sensitized Solar Cells with Catalytic Multiwall Carbon Nanotube Counter Electrodes. *ACS Appl. Mater. Interfaces* **2009**, *1*, 1145–1149.
20. Seo, S. H.; Kim, S. Y.; Koo, B. K.; Cha, S. I.; Lee, D. Y. Influence of Electrolyte Composition in the Photovoltaic Performance and Stability of Dye Sensitized Solar Cells with Multiwalled Carbon Nanotube Catalysts. *Langmuir* **2010**, *26*, 10341–10346.
21. Murakami, T. N.; Ito, S.; Wang, Q.; Nazeeruddin, M. K.; Bessho, T.; Cesar, I.; Liska, P.; Humphry-Baker, R.; Comte, P.; Pechy, P.; Grätzel, M. Highly Efficient Dye Sensitized Solar Cells Based on Carbon Black Counter Electrodes. *J. Electrochem. Soc.* **2006**, *153*, A2255–A2261.
22. Li, G.; Wang, F.; Jiang, Q.; Gao, X.; Shen, P. Carbon Nanotubes with Titanium Nitride as Low-Cost Counter Electrode for Dye Sensitized Solar Cells. *Angew. Chem., Int. Ed.* **2010**, *49*, 3653–3658.
23. Zukalova, M.; Prochazka, J.; Bastl, Z.; Duchoslav, J.; Rubacek, L.; Havlicek, D.; Kavan, L. Facile Conversion of Electrospun TiO_2 into Titanium Nitride/Oxynitride Fibers. *Chem. Mater.* **2010**, *22*, 4045–4055.
24. Banks, C. E.; Davies, T. J.; Wildgoose, G. G.; Compton, R. G. Electrocatalysis at Graphite and Carbon Nanotube Modified Electrodes: Edge-Plane Sites and Tube Ends Are the Reactive Sites. *Chem. Commun.* **2005**, 829–841.
25. Trancik, J. E.; Barton, S. C.; Hone, J. Transparent and Catalytic Carbon Nanotube Films. *Nano Lett.* **2008**, *8*, 982–987.
26. Sljukic, B.; Banks, C. E.; Compton, R. G. Iron Oxide Particles Are the Active Sites for Hydrogen Peroxide Sensing at Multiwalled Carbon Nanotube Modified Electrodes. *Nano Lett.* **2006**, *6*, 1556–1558.
27. Kim, K. S.; Zhao, Y.; Jang, H.; Lee, S. Y.; Kim, J. M.; Kim, K. S.; Ahn, J. H.; Kim, P.; Choi, J. Y.; Hong, B. H. Large-Scale Pattern Growth of Graphene Films for Stretchable Transparent Electrodes. *Nature* **2009**, *457*, 706–710.
28. Nair, R. R.; Blake, B.; Grigorenko, A. N.; Novoselov, K. S.; Booth, T. J.; Stauber, T.; Peres, N. M. R.; Geim, A. K. Fine Structure Constant Defines Visual Transparency of Graphene. *Science* **2008**, *320*, 1308.
29. Li, X.; Cai, W.; An, J.; Kim, S.; Nah, J.; Yang, D.; Piner, R.; Velamakanni, A.; Jung, I.; Tutuc, E.; Banerjee, S. K.; Colombo, L.; Ruoff, R. S. Large-Area Synthesis of High-Quality and Uniform Graphene Films on Copper Foils. *Science* **2009**, *324*, 1312–1314.
30. Wang, X.; Zhi, L.; Muellen, K. Transparent Conductive Graphene Electrodes for Dye Sensitized Solar Cells. *Nano Lett.* **2008**, *8*, 323–327.
31. Zhang, D. W.; Li, X. D.; Chen, S.; Li, H. B.; Sun, Z.; Yin, X. J.; Huang, S. M. Graphene Nanosheet Counter-Electrodes for Dye-Sensitized Solar Cells. In Proceedings of the 3rd International Nanoelectronics Conference, INEC 2010; Chu, P. K., Ed.; IEEE Press: Hong Kong, 2010; pp 610−611.
32. Choi, H.; Kim, H.; Hwang, S.; Choi, W.; Jeon, M. Dye Sensitized Solar Cells Using Graphene-Based Carbon Nano Composite as Counter Electrode. *Sol. Energy Mater. Sol. Cells* **2010**, *95*, 323–325.
33. Roy-Mayhew, J. D.; Bozym, D. J.; Punckt, C.; Aksay, A. Functionalized Graphene as a Catalytic Counter Electrode in Dye-Sensitized Solar Cells. *ACS Nano* **2010**, *10*, 6203–6211.
34. Hauch, A.; Georg, A. Diffusion in the Electrolyte and Charge-Transfer Reaction at the Platinum Electrode in Dye Sensitized Solar Cells. *Electrochim. Acta* **2001**, *46*, 3457–3466.
35. Chen, C. Y.; Wang, M.; Li, J. Y.; Pootrakulchote, N.; Alibabaei, L.; Cevey Ha, N. L.; Decoppet, J. D.; Tsai, J. H.; Grätzel, C.; Wu, C. G.; Zakeeruddin, S. M.; Grätzel, M. Highly Efficient Light-Harvesting Ruthenium Sensitizer for Thin Film Dye Sensitized Solar Cells. *ACS Nano* **2009**, *3*, 3103–3109.
36. Wenger, S.; Bouit, P. A.; Chen, Q.; Teuscher, J.; Di Censo, D.; Humphry-Baker, R.; Moser, J.; Delgado, J. L.; Martin, N.; Zakeeruddin, S. M.; Grätzel, M. Efficient Electron Transfer and Sensitizer Regeneration in Stable π-Extended Tetrathiafulvalene-Sensitized Solar Cells. *J. Am. Chem. Soc.* **2010**, *132*, 5164–5169.
37. Nazeeruddin, M. K.; Zakeeruddin, S. M.; Humphry-Baker, R.; Jirousek, M.; Liska, P.; Vlachopolous, N.; Shklover, V.; Fischer, C. H.; Grätzel, M. Acid Base Equilibria in Ruthenium(II) Complexes and the Effect of Protonation on Charge Transfer Sensitization of Nanocrystalline Titania. *Inorg. Chem.* **1999**, *38*, 6298–6305.